Second ordermagneticphasetransitionand scalinganalysisiniron doped manganiteLa0.7Ca0.3Mn1xFexO 3 compounds

by Kontan Tarigan

Submission date: 07-Apr-2019 02:49PM (UTC+0700)
Submission ID: 1107318239
File name: 2015-JMMM.pdf (2.58M)
Word count: 5164
Character count: 24052

Journal of Magnetism and Magnetic Materials 395 (2015) 41–47

Contents lists available at ScienceDirect

Journal of Magnetism and Magnetic Materials

journal homepage: www.elsevier.com/locate/jmmm

Second order magnetic phase transition and scaling analysis in iron doped manganite $La_{0.7}Ca_{0.3}Mn_{1-x}Fe_xO_3$ compounds

Dianta Ginting [a], Dwi Nanto [b], Yus Rama Denny [c], Kontan Tarigan [d], Syamsul Hadi [e], Mohammad Ihsan [f,g], Jong-Soo Rhyee [a,*]

[a] Department of Applied Physics and Institute of Natural Sciences, Kyung Hee University, Yong-in 446-701, South Korea
[b] Physics Education, Syarif Hidayatullah State Islamic University, Jakarta 15412, Indonesia
[c] Department of Electrical Engineering, University of Sultan Ageng Tirtayasa, Banten 42435, Indonesia
[d] Department of Mechanical Engineering, Mercu Buana University, Jakarta-Barat, Jakarta 11650, Indonesia
[e] Department of Mechanical Engineering, State Polytechnic of Malang, East Java 65100, Indonesia
[f] PSTBM-BATAN, Kawasan Puspiptek Serpong, Tangerang Selatan, Banten 15314, Indonesia
[g] Institute of Electronic Materials, University of Wollongong, Wollongong NSW 2522, Australia

ARTICLE INFO

Article history:
Received 27 March 2015
Received in revised form
18 May 2015
Accepted 12 July 2015
Available online 14 July 2015

Keywords:
Second order magnetic transition
Critical behaviors
Iron doped
Manganite
Perovskite

ABSTRACT

We investigated magnetic properties of $La_{0.7}Ca_{0.3}Mn_{1-x}Fe_xO_3$ ($x=0.09$ and 0.11) compounds in terms of isothermal magnetization analysis and scaling behavior with various critical exponents. From the Landau theory of magnetic phase transition, we found that the paramagnetic to ferromagnetic phase transition in $La_{0.7}Ca_{0.3}Mn_{1-x}Fe_xO_3$ ($x=0.09$ and 0.11) compounds is the type of second order magnetic transition (SOMT), which contrary to the first order magnetic transition (FOMT) for low Fe-doped compounds ($x<0.09$) in previous reports. When we investigate the critical behavior of the compounds near $T=T_c$ by the modified Arrott plot, Kouvel–Fisher plots, and critical isothermal analysis, the estimated critical exponents β, γ, and δ are in between the theoretically predicted values for three-dimensional Heisenberg and mean-field interaction models. It is noteworthy that the scaling relations are obeyed in terms of renormalization magnetization $m=\varepsilon^{-\beta}M(H,\varepsilon)$ and renormalized field $h=\varepsilon^{\beta+\gamma}H$. Temperature-dependent effective exponents β_{eff} and γ_{eff} correspond to the ones of disordered ferromagnets. It is shown that the magnetic state of the compounds is not fully described by the conventional localized-spin interaction model because the ferromagnetic interaction has itinerant character by increasing Fe-doping concentration.

1. Introduction

There have been much interest in hole-doped perovskite manganites of $R_{1-x}A'_xMnO_3$ (R=La, Pr, Nd; A′=Pb, Ca, Sr etc.) due to their colossal mangnetoresistance (CMR) and many other interesting magnetic properties near the ferromagnetic–paramagnetic (FM–PM) phase-transition temperature [1]. Basically, the CMR is usually explained by means of the double-exchange (DE) mechanism between Mn^{3+} and Mn^{4+} ions. The strong electron–phonon coupling in manganites gives rise to the Jahn–Teller distortion [2,3]. Magnetic and magnetotransport properties thus depend not only on the Mn^{3+}/Mn^{4+} ratio but also on the bond length and bond angle of the perovskite structure. Among perovskite manganites, $La_{0.7}Ca_{0.3}Mn_{1-x}Fe_xO_3$ has received special interest because they showed both CMR and giant magnetocaloric (GMC) effects [4,5].

Here, we investigated the magnetic properties of $La_{0.7}Ca_{0.3}Mn_{1-x}Fe_xO_3$ ($x=0.09$ and $x=0.11$) compounds. In a previous report, it was reported the first order magnetic transition in low Fe-doped $La_{0.7}Ca_{0.3}Mn_{1-x}Fe_xO_3$ ($x=0$–0.07) compounds [5] and the critical exponents found to be far from the expected values from theoretical model [6].

According to the Landau theory of magnetic phase transition [7], we can distinguish the type of magnetic phase transition, such as the first-order (FOMT) and second-order magnetic transitions (SOMT). By analyzing the magnetic properties, we found the SOMT in the $La_{0.7}Ca_{0.3}Mn_{1-x}Fe_xO_3$ compounds for Fe doping at the doping ratios of $x=0.09$ and $x=0.11$. In addition, the critical exponents on the compounds have unconventional characteristics. For example, the critical exponents do not correspond to the conventional universality class with mean field theory and

* Corresponding author.
E-mail address: jsrhyee@khu.ac.kr (J.-S. Rhyee).

http://dx.doi.org/10.1016/j.jmmm.2015.07.033
0304-8853/

Heisenberg model. On the other hand, the critical exponents obey scaling relations near the T_c. The effective exponents (β_{eff}, γ_{eff}) vary with temperature similar to those from renormalized group approach [8].

2. Experiments

Polycrystalline samples of $La_{0.7}Ca_{0.3}Mn_{1-x}Fe_xO_3$ (x=0.09 and 0.11) were prepared by conventional solid-state reaction method. Stoichiometric mixture of high-purity powders of La, $CaCO_3$, Fe_2O_3, and $MnCO_3$ were ground, mixed well, and then calcined in air at 1000 °C for 24 h. The calcined powders were cold pressed and sintered at 1300 °C for 24 h in air. After grinding and repeating the sintering processes, the crystal structure of the final products was investigated by the X-ray diffractometer (Brucker AXS, D8 Discover). Magnetic measurements were performed on a vibrating sample magnetometer (VSM) with the magnetic-field range of 0–10 kOe.

3. Results and discussion

The crystal structure of $La_{0.7}Ca_{0.3}Mn_{1-x}Fe_xO_3$ (x=0.09 and 0.11) samples was examined by an X-ray diffractometer in an angle range of 20–70° which is shown in Fig. 1. It shows single phase of the orthorhombic structure with *Pbnm* space group with no noticeable impurities. The lattice parameters of the compounds are a=5.451(6) Å, b=7.700(4) Å, and c=5.446(7) Å which is not significantly different with each other due to small doping variation.

The temperature dependence of magnetization $M(T)$ is shown in Fig. 2 for $La_{0.7}Ca_{0.3}Mn_{0.91}Fe_{0.09}O_3$ under a magnetic field of H=50 Oe. The low field magnetization shows the ferromagnetic transition. The Curie temperature is defined by the extreme of dM/dT vs. T as shown in the inset of Fig. 2, which is obtained by T_c =107.71 K for x=0.09 and T_c=103.28 K for x=0.11, respectively. However, a more accurate $T_c|_{H=0}$ values could be determined by using the analysis of the critical exponents from the isothermal magnetization curves around T_c, as shown in Fig. 3(a) and (b). The figures show magnetic-field dependences of magnetization, $M(H)$, for $La_{0.7}Ca_{0.3}Mn_{0.91}Fe_{0.09}O_3$ and $La_{0.7}Ca_{0.3}Mn_{0.89}Fe_{0.11}O_3$ at various temperatures as indicated with a temperature step of 2 K. In the temperature range of $T<T_c$, the magnetization increases nonlinearly with increasing the magnetic field, but the saturation magnetization is not attained. Meanwhile, in the region $T>T_c$, M (H) shows linear increase with increasing magnetic fields.

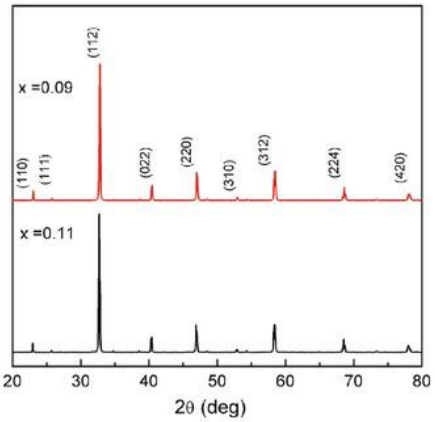

Fig. 1. X-ray diffraction patterns of $La_{0.7}Ca_{0.3}Mn_{1-x}Fe_xO_3$ (x=0.09 and 0.11).

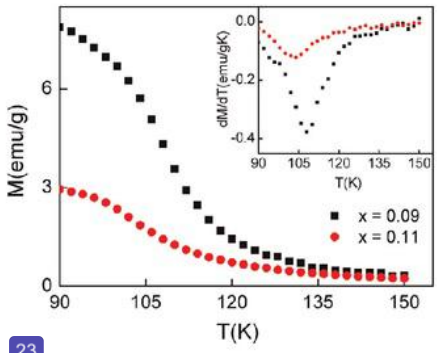

Fig. 2. The temperature dependence of magnetization for $La_{0.7}Ca_{0.3}Mn_{1-x}Fe_xO_3$ (x=0.09 and 0.11) under a magnetic field of H=50 Oe. The Curie temperature corresponding to the extreme of dM/dT vs. T (inset).

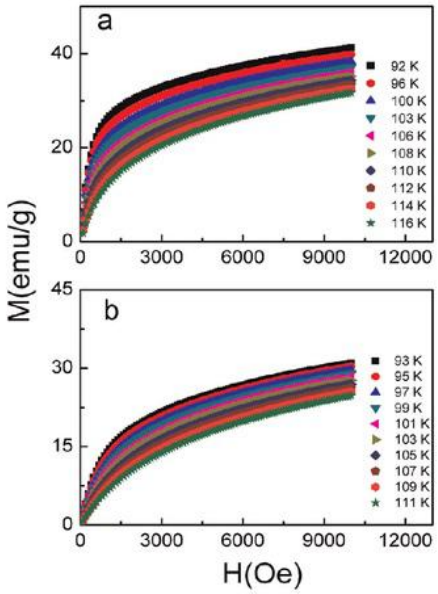

Fig. 3. Magnetization vs. magnetic field M–H curves for $La_{0.7}Ca_{0.3}Mn_{1-x}Fe_xO_3$ with (a) x=0.09 and (b) x=0.11.

For a ferromagnetic materials, the magnetization can be represented by a scaled equation of state, which is led from a scaling hypothesis. Scaling hypothesis or, equivalently, the homogeneity postulate makes two specific predictions: (i) it relates various critical exponents through scaling, (ii) it makes specific predictions concerning the form of the equation of state. According to the scaling hypothesis, for SOMT, the spontaneous magnetization M_s (T) below T_c, inverse initial susceptibly $\chi_0^{-1}(T)$ above T_c, and magnetization M at T_c show following power law dependence [9]:

$$M_s(T) = M_0(-\varepsilon)^{\beta}, \quad \varepsilon < 0, \tag{1}$$

$$\chi_0^{-1}(T) = (h_0/M_0)\varepsilon^{\gamma}, \quad \varepsilon > 0, \tag{2}$$

$$M = DH^{1/\delta}, \quad \varepsilon = 0, \tag{3}$$

where M_0, h_0, and D are critical amplitudes of magnetization, magnetic field, and coefficient of critical behavior of magnetization, respectively, $\varepsilon=(T-T_c)/T_c$ is the reduced temperature and β, γ, and δ are the critical exponents. The magnetic equation of state is a relationship among the variables M (H,ε), H, and T. Using scaling

hypothesis this can be expressed as

$$M(H, \varepsilon) = |\varepsilon|^{\beta} f_{\pm}(H/|\varepsilon|^{\beta+\gamma}), \quad (4)$$

where f_+ for $T > T_c$ and f_- for $T < T_c$ are regular analytic functions. In terms of renormalization of magnetization $m = \varepsilon^{-\beta} M(H,\varepsilon)$ and magnetic field $h = |\varepsilon|^{\beta+\gamma} H$, the Eq. (4) can be written as

$$m = f_{\pm}(h) \quad (5)$$

Eq. (5) implies that for an appropriate choice of critical exponents, scaled m plotted as a function of scaled h will fall on two universal curves: one above T_c and another below T_c.

Generally, the critical exponents and critical temperature can be easily determined by analyzing the Arrott plot at temperatures around T_c [10,11]. In the Landau theory of phase transition, the Gibbs free energy G can be expressed in terms of the order parameter M as

$$G(T, M) = G_0 + aM^2 + bM^4 - MH \quad (6)$$

where the coefficients a and b are temperature-dependent [12]. For an equilibrium state ($dG/dM = 0$), the magnetic equation of state transforms into:

$$\frac{H}{M} = 2a + 4bM^2 \quad (7)$$

Thus, M^2 vs. H/M should appear as straight lines in the high field range in the Arrott plot. The intercept of M^2 as a function of H/M on the H/M axis is negative (positive) below (above) T_c. The lines of M^2 vs. H/M at T_c should cross the origin.

According to the criterion of Landau theory [7], the order of magnetic transition can be determined from the slope of the straight line in the Arrott's plot: the positive slope corresponds to the second order magnetic transition (SOMT) while the negative slope corresponds to the first order magnetic transition (FOMT). Fig. 4(a) and (b) show the Arrott plot of M^2 vs. H/M for the $La_{0.7}Ca_{0.3}Mn_{1-x}Fe_xO_3$ ($x = 0.09$ and 0.11) around T_c. The positive slope of M^2 vs. H/M plot indicates that the PM–FM phase transition

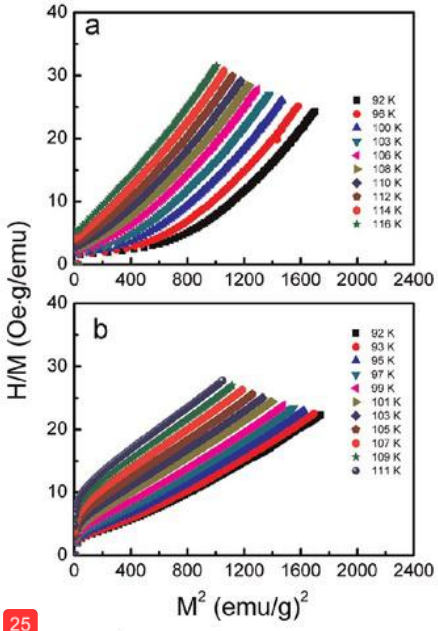

Fig. 4. The Arrott plot of M^2 vs. H/M for $La_{0.7}Ca_{0.3}Mn_{1-x}Fe_xO_3$ with (a) $x = 0.09$ and (b) $x = 0.11$ near T_c.

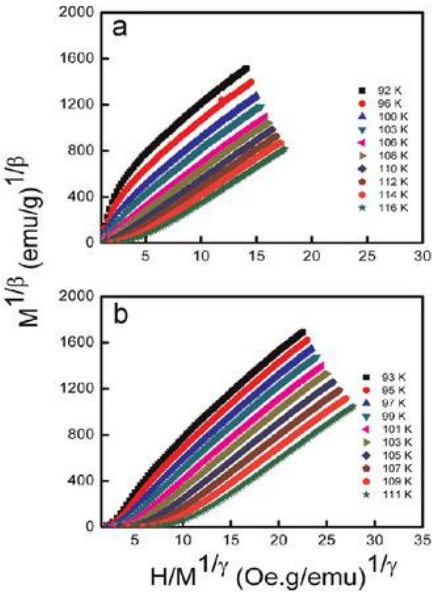

Fig. 5. Modified Arrott plots of $M^{1/\beta}$ vs. $(H/M)^{1/\gamma}$ for $La_{0.7}Ca_{0.3}Mn_{1-x}Fe_xO_3$ with (a) $x = 0.09$ and (b) $x = 0.11$ near T_c.

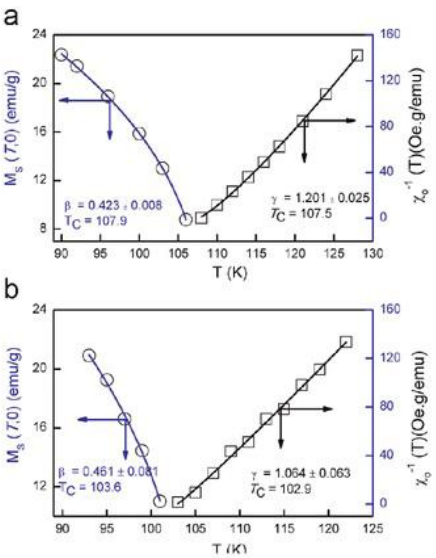

Fig. 6. Temperature dependences of $M_S(T)$ and $\chi_0^{-1}(T)$, together with the fitting curves based on the critical laws with Fe-doping concentrations of $La_{0.7}Ca_{0.3}Mn_{1-x}Fe_xO_3$ (a) $x = 0.09$ and (b) $x = 0.11$.

is a type of SOMT.

However, all curves in the Arrott plot are nonlinear and show upward curvature even in the high-field region, which indicates that $\beta = 0.5$ and $\gamma = 1$ are not satisfied according to the Arrott–Noakes equation of state $(H/M)^{(1/\gamma)} = (T - T_c)/T_c + (M/M_1)^{1/\beta}$, where M_1 is a characteristic constant depending on materials [13]. In other words, the Landau theory of phase transition or the mean field theory with $\beta = 0.5$ and $\gamma = 1$ is not valid for the $La_{0.7}Ca_{0.3}Mn_{0.91}Fe_{0.09}O_3$ and $La_{0.7}Ca_{0.3}Mn_{0.89}Fe_{0.11}O_3$ compounds.

Thus, the modified Arrott plots are employed to obtain the

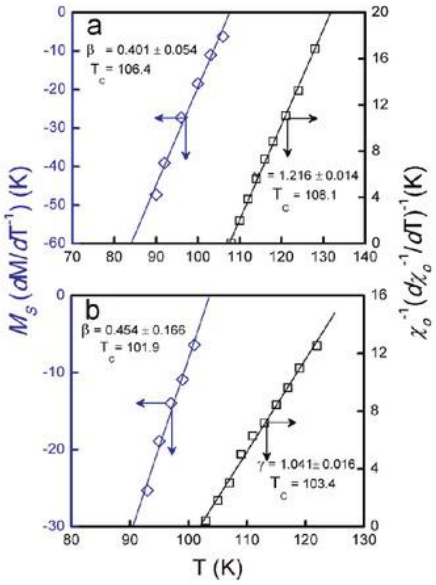

Fig. 7. Kouvel–Fisher plot for the spontaneous magnetization M_S and for the inverse the initial susceptibility χ_0^{-1} of $La_{0.7}Ca_{0.3}Mn_{1-x}Fe_xO_3$ (a) $x=0.09$ and (b) $x=0.11$.

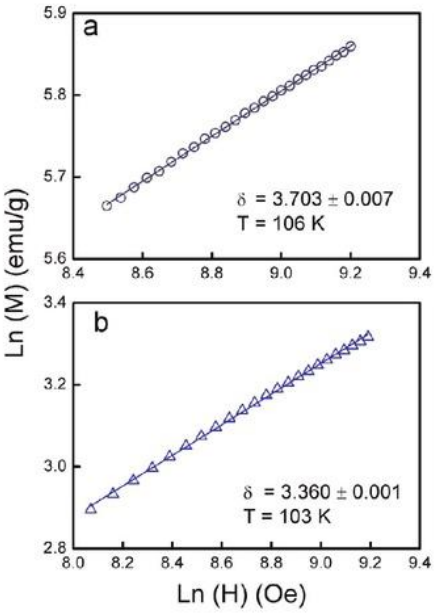

Fig. 8. Log–log plot of critical isotherms for $La_{0.7}Ca_{0.3}Mn_{1-x}Fe_xO_3$ (a) $x=0.09$ and (b) $x=0.11$.

correct critical exponents β and γ. This is given by following equation of state:

$$(H/M)^{(1/\gamma)} = a(T-T_c)/T_c + bM^{1/\beta}, \quad (8)$$

where a and b are considered to be constants which represents modified Arrott plot in the Eq. (8) for the $La_{0.7}Ca_{0.3}Mn_{0.91}Fe_{0.09}O_3$ and $La_{0.7}Ca_{0.3}Mn_{0.89}Fe_{0.11}O_3$ compounds at different temperatures. If we choose proper β and γ, the isothermal plot can clearly be shown as parallel straight lines at high fields.

However, the selection of exponents β and γ is nontrivial from Eq. (8) as shown in Fig. 5. To overcome this difficulty, a rigorous iterative method has been employed to find out the appropriate values of β and γ. In this method, starting trial values of β and γ are taken for theoretical 3-D Heisenberg model. When we substitute these values of β and γ in Eq. (8), we obtained a similar behavior with Fig. 5 (not shown). Linear extrapolation of the isotherms is taken from the high field which gives $(M_s)^{1/\beta}$ and $(\chi_0^{-1})^{1/\gamma}$ as an intercept on $(M)^{1/\beta}$ and $(H/M)^{1/\gamma}$ axis, respectively. These values of $M_s(T)$ and $\chi_0^{-1}(T)$ have been used in Eqs. (1) and (2), respectively. According to Eq. (1), the slope of the straight line fitting of log $[M_s(T)]$ vs. log (ε) gives a value of β. Similarly, the straight line fitting of log $[\chi_0^{-1}(T)]$ vs. log (ε) from Eq. (2), will give new γ. For fitting the straight lines, the T_c in Eqs. (1) and (2) is adjusted as a free parameter so as to give best fitting. These new values of β and γ are again in used to construct new modified Arrott plot in Fig. 5 (a) and (b). This process was continued until when the values of, β, γ, *and* T_c are stably converged.

From the iterative calculation, a set of reasonably good parallel straight lines have been generated with values of $\beta=0.423$, $\gamma=1.201$ for $x=0.09$ and $\beta=0.461$, $\gamma=1.201$ for $x=0.11$, respectively. It is evident that the modified Arrott plot does not show linear behavior at low magnetic field region as shown in Fig. 5 (a) and (b) because the direction of magnetization are randomly oriented in low magnetic field region [14]. On the other hand, in high fields, all isothermal scaled magnetization are set of parallel straight lines. The intercept of linear extrapolation from high magnetic field of the isothermal scaled magnetization passes through the origins at $T_c=107.75$ K for $x=0.09$ and at 103.28 K for $x=0.11$, respectively.

The calculated values of temperature-dependent saturation magnetization $M_s(T)$ and inverse initial magnetic susceptibility $\chi_0^{-1}(T)$ are plotted in Fig. 6(a) and (b), respectively. Using these values of $M_s(T)$ and $\chi_0^{-1}(T)$, Eq.(1) gives $\beta=0.423$ and $T_c=107.94$ K for $x=0.09$ and $\beta=0.461$ and $T_c=103.63$ K for $x=0.11$, respectively. Also, Eq. (2) gives $\gamma=1.201$ and $T_c=107.56$ K for $x=0.09$ and

Table 1
Values of the exponents β, γ, δ as determined from the Arrott plots, Kouvel–Fisher plot for $La_{0.7}Ca_{0.3}Mn_{1-x}Fe_xO_3$ ($x=0.09$ and 0.11). The theoretically predicted values of exponents for various universality are given for the sake of comparison.

Material	Technique	T_c(K)	β	γ	δ	Ref.
$La_{0.7}Ca_{0.3}Mn_{0.91}Fe_{0.09}O_3$	Modified Arrott plot	107.75	0.423 ± 0.008	1.201 ± 0.025	3.70 ± 0.07 3.83 ± 0.016[a]	This work
	Kouvel–Fisher method	107.27	0.401 ± 0054	1.216 ± 0.014	4.03 ± 0.034[a]	This work
$La_{0.7}Ca_{0.3}Mn_{0.89}Fe_{0.11}O_3$	Modified Arrott plot	103.28	0.461 ± 0.081	1.064 ± 0.063	3.36 ± 0.01 3.30 ± 0.072[a]	This work
	Kouvel–Fisher method	103.46	0.450 ± 0.166	1.041 ± 0.016	3.31 ± 0.091[a]	This work
Mean field model	Theory	–	0.5	1.0	3.0	[15]
3D Heisenberg Model	Theory	–	0.365	1.386	4.80	[15]
3D Ising Model	Theory	–	0.325	1.241	4.82	[15]

[a] Calculated from widom scaling relation $\delta = 1+\gamma/\beta$.

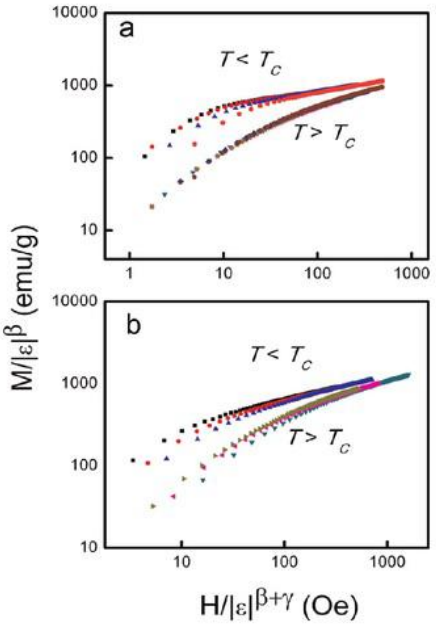

Fig. 9. Scaling plot for $La_{0.7}Ca_{0.3}Mn_{1-x}Fe_xO_3$ (a) $x=0.09$ and (b) $x=0.11$, indicating the two universal curves below and above T_c.

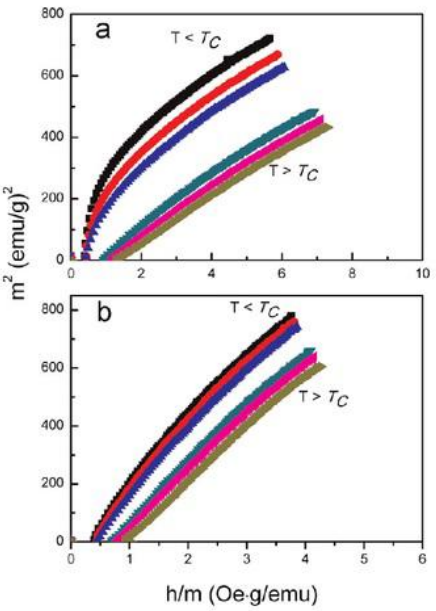

Fig. 10. The renormalized-magnetization and field are plotted in the form of m^2 vs. h/m for $La_{0.7}Ca_{0.3}Mn_{1-x}Fe_xO_3$ (a) $x=0.09$ and (b) $x=0.1$. The plots show all data collapse into two separate branches: one below T_c and another above T_c.

$\gamma=1.064$ and $T_c=102.94$ K for $x=0.11$, respectively. From this analysis with the criteria, we can define the critical temperature as an averaged values of $T_c=107.75$ K for $x=0.09$ and $T_c=103.28$ K for $x=0.02$.

Alternatively, the values of β and γ can be obtained also by the Kouvel–Fisher (K–F) method [15]. According to this method the plots of $M_s(dM_s/dT)^{-1}$ and $\chi_0^{-1}(T)$ $(d\chi_0^{-1}/dT)^{-1}$ vs. T should yield straight lines with slopes of $1/\beta$ and $1/\gamma$, respectively. When the data are extrapolated to ordinate equal zero, the intercept of straight lines on T axis equals to T_c. The Kouvel–Fisher plots are shown in Fig. 7(a) and (b). The straight lines obtained from a least-square fit to the data give the values of $\beta=0.401$, $\gamma=1.216$ and $T_c=107.275$ K for $x=0.09$, $\beta=0.454$, $\gamma=1.04$ and $T_c=102.665$ K for $x=0.11$, respectively. It is remarkable that the values of critical exponents as well as T_c calculated using both modified of Arrott and Kouvel–Fisher plots give reasonably similar values (see Table 1), indicating the self-consistent analysis.

The another critical exponent δ can be determined directly from the critical isothermal analysis of $M(T_c, H)$. According to Eq. 3, ln (M) vs. ln (H) would give rise to the straight lines with a slope of $1/\delta$. From the linier fitting of ln (M) vs. ln (H) plot in Fig. 8(a) and (b), we get the value of $\delta=3.70$ at $T=106$ K for $x=0.09$ and $\delta=3.30$ at $T=103$ K for $x=0.11$, respectively, which is presented in Table 1. These values are very close to $\delta=3.83$ for $x=0.01$ and $\delta=3.30$ for $x=0.11$ determined from the Widom scaling relation [16]:

$$\delta = 1 + \gamma/\beta. \tag{9}$$

Hence, estimated exponents (β, γ) in present study are self-consistent and an accurate within the experimental precision.

We have then compared our data with the prediction of scaling theory. According to Eq. (4), the functional analysis of $M|\varepsilon|^{\beta}$ with $H/|\varepsilon|^{(\beta+\gamma)}$ produces two universal curves, one for temperatures below T_c, and the other one for above T_c. Using the values of β and γ obtained above, the scaled data for the samples $x=0.09$ and 0.11 are plotted in Fig. 9(a) and (b), respectively. The high-field data points fall on two functional forms for $T<T_c$ and $T>T_c$. In other words, the $La_{0.7}Ca_{0.3}Mn_{1-x}Fe_xO_3$ samples undergo SOMT. It is noteworthy that the scaling behavior at high temperature is better than the one of low-magnetic fields due to rearrangement of magnetic domains and the effect of the uncertainty in the calculation of demagnetization factor which become significant in low field region.

The reliability of the exponents and T_c has been further ensured with more rigorous analysis by plotting m^2 vs. h/m [17]. Fig. 10 (a) and (b) also show two functional behaviors: one below T_c and the other above T_c. This proves that the critical parameters determined in our work are in good accordance with the scaling hypothesis.

If there is various competing couplings and randomness in a magnetic system, then the critical behavior may have various systematic trends or crossover phenomena. In that case, it is useful to generalize as a power law for the critical behavior by defining effective exponents as follows:

$$\beta_{eff} = -\frac{d(\ln M_s(\varepsilon))}{d(\ln \varepsilon)} \tag{10}$$

$$\gamma_{eff} = -\frac{d(\ln \chi_0(\varepsilon))}{d(\ln \varepsilon)} \tag{11}$$

In usual cases, exponents in the asymptotic regime $(\varepsilon \to 0)$ show universal properties. In other words, the critical behaviors depend on the macroscopic bulk parameters of the system such as symmetry and dimensionality of the order parameters which are independent of the microscopic details of the samples. However, in some cases, exponents often show various systematic behaviors or crossover phenomenon as $T \to T_c$ [18,19].

Even through the estimated critical exponents in present study strictly do not belong to the usual universality classes, it is important to find out the universality that approaches to the one in the asymptotic limit. For this purpose, we calculate the effective exponent β_{eff} and γ_{eff} as a function of ε with Eq. (10) which are presented in Fig. 11. Fig. 11(a) and (b) represents β_{eff} and (c) and (d) represent γ_{eff} for $x=0.09$ and 0.11 compounds, respectively. As

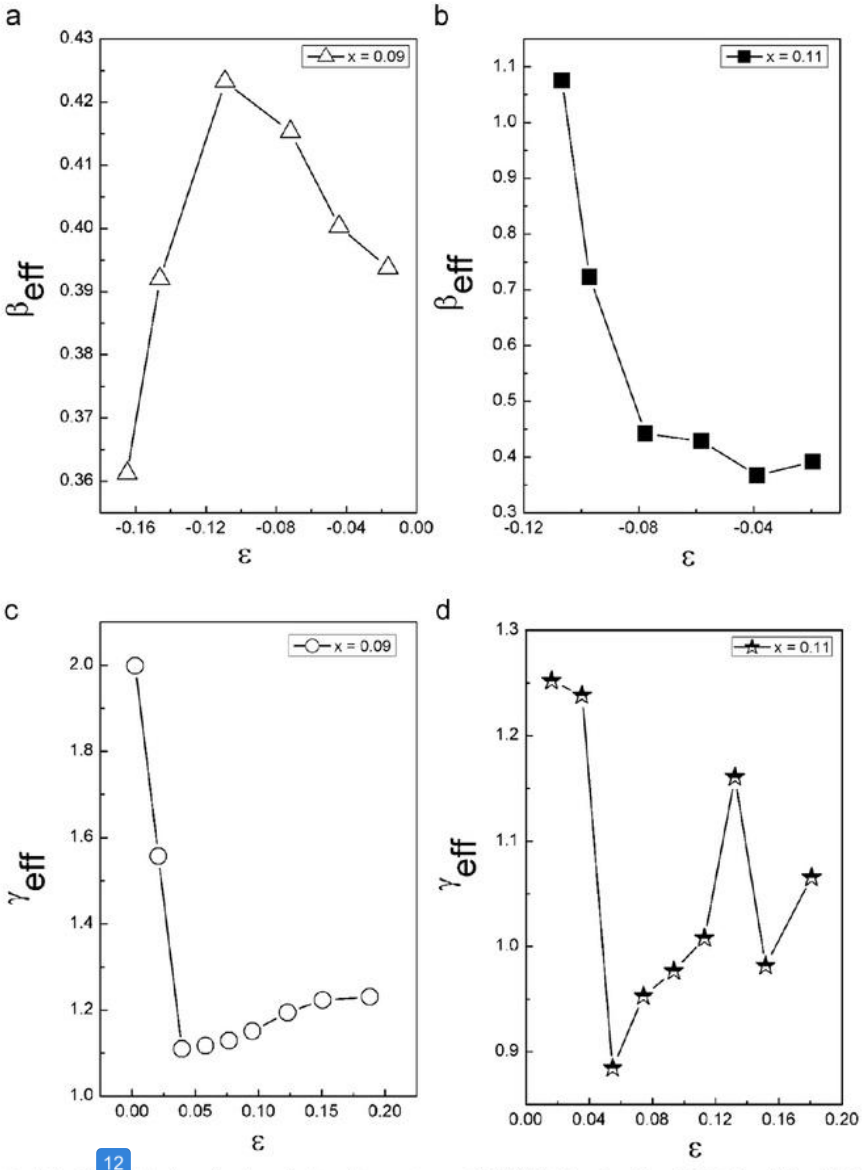

Fig. 11. Effective exponent β_{eff} below T_c are plotted as a function of reduced temperature $\varepsilon=(T-T_c)/T_c$ for $La_{0.7}Ca_{0.3}Mn_{1-x}Fe_xO_3$ (a) $x=0.09$ and (b) $x=0.11$. Effective exponent γ_{eff} above T_c are plotted as a function of reduced temperature $\varepsilon=(T-T_c)/T_c$ for $La_{0.7}Ca_{0.3}Mn_{1-x}Fe_xO_3$ (c) $x=0.09$ and (d) $x=0.11$.

in the Fig. 11(a) and (b), the β_{eff} shows non-monatomic change with ε. For $x=0.09$ compound, the β_{eff} shows increased from $\beta_{eff} \approx 0.393$ at $\varepsilon \approx -0.016$ to the maximum value of $\beta_{eff} \approx 0.423$ at $\varepsilon \approx -0.104$ with following decrease of β_{eff} to the value of 0.3655 at $\varepsilon \approx -0.034$. In the case of $x=0.11$ compound, the $\beta_{eff} \approx 1.06$ at $\varepsilon \approx -0.107$decreases with increasing ε. On the other hand, the γ_{eff} is decreased significantly from $\gamma_{eff} \approx 1.982$ at $\varepsilon \approx 0.02$ to the dip point of $\gamma_{eff} \approx 1.109$ at $\varepsilon \approx 0.040$ with slight increase of γ_{eff} with increasing ε for $x=0.09$ compound. For $x=0.11$ compound, the γ_{eff} shows irregular behavior with ε.

The unusual behavior of critical exponents might be raised by several possible reasons; (i) ε_{min} does not fall into the asymptotic exponents; (ii) the materials have disorder because the disagreement of effective exponents with universality classes in asymptotic regime is also observed in disorder materials [20]; (iii) the system goes through crossover regime to another universality class in asymptotic regime [21].

While the low Fe-doped compounds of $La_{0.7}Ca_{0.3}Mn_{1-x}Fe_xO_3$ ($0.0 \le x \le 0.07$) exhibit first order magnetic transition [5], we found the second order magnetic transition for the present compound of $La_{0.7}Ca_{0.3}Mn_{1-x}Fe_xO_3$ ($x=0.09$ and 0.11) under the critical behavior investigation. The second order magnetic transition was also observed in the homologous compounds of $La_{0.67}Ca_{0.33}Mn_{0.9}Fe_{0.1}O_3$ [21] and $La_{0.67}Ca_{0.33}Mn_{0.9}Ga_{0.1}O_3$ [22].

The SOMT by Fe ions implies the weakening of magnetic interaction. It is well known that the magnetic interaction of manganites is double exchange or superexchange interaction. Ahn et al. [23] described that Mn $e_g(\uparrow)$ band is electronically active, where electrons hop between the Mn^{3+} and Mn^{4+} ions. The substitution of Fe^{3+} ions at Mn^{3+} ionic sites in $La_{0.7}Ca_{0.3}Mn_{1-x}Fe_xO_3$ at $x=0.09$ and $x=0.11$ compounds can reduce the number of available hopping sites, resulting in the

suppression of double exchange interaction, which gives rise to the reduction of ferromagnetic exchange and metallic conduction. Moreover, Mn–O–Mn and Fe–O–Fe chains coexist that reinforces magnetic inhomogeneity. Cai et al. [24] observed ferromagnetic clusters embedded in antiferromagnetism for $La_{0.67}Ca_{0.33}Mn_{0.9}Fe_{0.1}O_3$ compound from the suppression of double exchange (DE) interaction. The competition between the ferromagnetic DE interaction and the coexistence of antiferromagnetic super-exchange interaction with the introduction of Fe^{3+} for Mn^{3+} gives rise to the randomly canted ferromagnetic state at low temperature. In addition, the variation in structural parameters, particularly for the Mn–O bond length and Mn–O–Mn bond angle [25], influences directly to the magnetic phase transition in $La_{0.7}Ca_{0.3}Mn_{1-x}Fe_xO_3$ at $x<0.09$.

Table 1 shows the critical exponents of $La_{0.7}Ca_{0.3}Mn_{1-x}Fe_xO_3$ ($x=0.09$ and $x=0.11$) obtained from modified Arrott plot and Kouvel–Fisher method and the theoretical expectations. It is clear that with increasing Fe contents, the values of critical exponent β is increased while γ is decreased. To explain the critical exponents obtained for $La_{0.7}Ca_{0.3}Mn_{1-x}Fe_xO_3$ ($x=0.09$ and $x=0.11$), we have compared the values of the theoretical models and earlier studies on manganites. In our case, the values of $\beta=0.423\pm0.008$ for $x=0.09$ and $\beta=0.461\pm0.081$ for $x=0.11$ are in between to that expected for the mean-field (MF) theory ($\beta=0.5$) and Heisenberg model ($\beta=0.365$), this behavior was also observed in $La_{0.7}Sr_{0.3}Mn_{0.97}Ni_{0.03}O_3$ ($\beta=0.468$) [15]. On the other hand, the values of $\gamma=1.201\pm0.025$ for $x=0.1$ are close to 3-D Ising model with $\gamma=1.241$ and $\gamma=1.064\pm0.063$ for $x=0.11$ are closed to the predicted value for the MF theory with $\gamma=1$.

These results prove that FM interactions in $La_{0.7}Ca_{0.3}Mn_{1-x}Fe_xO_3$ ($x=0.09$ and $x=0.11$) have the following properties: (i) it does not comply with a short-range interaction model; (ii) the estimated exponents are in between the values expected for the 3-D Heisenberg and MF models, indicating the magnetic interactions are extended type; and (iii) it has an itinerant characteristic. It is known that the values of the critical exponents depend strongly on the range of exchange interaction $J(r)$, spins and the spatial dimensionality. Fisher et al. [8] showed that the critical exponents approach to the values of Heisenberg model if the exchange interaction has the form of $J(r)=1/r^{d+\sigma}$ (d is the spatial dimension of the system and σ is the range of the interaction). If $\sigma\geq2$, then the Heisenberg exponents with $\beta=0.365$, $\gamma=1.386$ and $\delta=4.8$ are valid. The mean-field exponents with $\beta=0.5$, $\gamma=1$ and $\delta=3$ are valid for σ less than 3/2. For $\frac{1}{2}<\sigma<2$, the exponents belong to other universality classes which depend on σ. Thus, these results suggest that critical phenomena in $La_{0.7}Ca_{0.3}Mn_{1-x}Fe_xO_3$ ($x=0.09$ and $x=0.11$) could not be explained on the conventional universality classes.

4. Conclusion

We have studied the influence of Fe-doping on the critical properties of polycrystalline samples of $La_{0.7}Ca_{0.3}Mn_{1-x}Fe_xO_3$ ($x=0.09$ and $x=0.11$) prepared by solid-state reaction. The critical behavior of magnetization at paramagnetic (PM) to ferromagnetic (FM) phase transition in $La_{0.7}Ca_{0.3}Mn_{1-x}Fe_xO_3$ ($x=0.09$ and $x=0.11$) was studied using the modified Arrott plot, Kouvel–Fisher plot, and critical isotherm analysis. From the analysis, we found that the PM to FM phase transition is of the second order on the doping range.

The critical exponents β, γ, and δ estimated from various techniques reasonably correspond to the values in between those theoretically predicated values from 3-D Heisenberg and mean-field (MF) interaction models. Even though the critical exponents are in between 3-D Heisenberg and MF theory, the isothermal field-dependent magnetization at various temperatures $M(H,T)$ follow the scaling behavior around T_c, which falls into two functional branches of a universal function $M(H,\varepsilon)=|\varepsilon|^{\beta}f_{\pm}(H/|\varepsilon|^{\beta+\gamma})$, where $\varepsilon=(T-T_c)/T_c$ is the reduced temperature and f_+ (f_-) represents the function at $T>T_c$ ($T<T_c$). This conclusively shows that calculated critical exponets as well as critical temperature are obtained reasonably to the system. The γ_{eff} is increasing with increase of ε for $x=0.09$ compound. For $x=0.11$ compound, the γ_{eff} shows irregular behavior with ε.

Acknowledgment

This work is supported by the Samsung Future Technology Center.

References

[1] A.J. Millis, B.I. Shraiman, R. Mueller, Phys. Rev. Lett. 77 (1996) 175.
[2] C. Zener, Phys. Rev. 82 (1951) 403.
[3] A.J. Millis, P.B. Littlewood, B.I. Shraiman, Phys. Rev. Lett. 74 (1995) 5144.
[4] L. Kumar, H. Kishan, A. Rao, V.P.S. Awana, J. Alloy Compd. 502 (2010) 283.
[5] D. Kampen, Y. Zhang, T.L. Phan, P. Zhang, S.C. Yu, H. Srikanth, M.H. Phan, J. Phys. 112 (2012) 113901.
[6] H.S. Shin, J.E. Lee, Y.S. Nam, H.L. Ju, C.W. Park, J. Sci. Commun. 118 (2001) 377.
[7] S.K. Banerjee, Phys. Lett. 12 (1964) 16.
[8] M.E. Fisher, S.K. Ma, B.G. Nickel, Phys. Rev. Lett. 29 (1972) 917.
[9] H.E. Stanley, Introduction to Phase Transitions and Critical Phenomena, Oxford University Press, London, 1971.
[10] A. Arrott, Phys. Rev. 108 (1957) 1394.
[11] J. Yeung, M.R. Roshko, G. Williams, Phys. Rev. B34 (1986) 3456.
[12] K.H. Yu, Magnetism and Superconductivity, Springer, Berlin, 2002.
[13] A. Arrott, J.E. Noakes, Phys. Rev. Lett. 19 (1967) 786–789.
[14] A. Aharoni, Introduction to the Theory of Ferromagnetism, Clarendon Press, Oxford, 1996, chap. 4.
[15] D. Ginting, D. Nanto, Y.D. Zhang, S.C. Yu, T.L. Phan, Physica B 412 (2013) 17.
[16] E.W. Bohm, J. Chem. Phys. 43 (1965) 3898.
[17] S.N. Kaul, J. Magn. Magn. Mater. 53 (1985) 5.
[18] A. Venimadhaval, V. Srinivas, V.V. Rao, R.A. Dunlap, Phys. Rev. Lett. 91 (2003) 137202.
[19] S. Mukherjee, S.N. Kaul, M.K. Sostarich, Phys. Rev. B 62 (2000) 11649.
[20] M. Dudka, R. Folk, Y. Holovatch, D. Ivaneiko, J. Magn. Magn. Mater. 256 (2003) 102.
[21] D.C. Kundaliya, R. Vij, R.G. Kulkarni, A.A. Tulapukar, R. Pinto, S.K. Malik, W. B. Yelon, J. Magn. Magn. Mater. 264 (2003) 62.
[22] S. Rößler, U.K. Rößler, K. Nenkov, D. Eckert, S.M. Yusuf, K. Dörr, K.H. Müller, Phys. Rev. B 70 (2004) 104417.
[23] K.H. Ahn, X.W. Wu, K. Liu, C.L. Chien, Phys. Rev. B 54 (1996) 15299.
[24] J.W. Cai, C. Wang, B.G. Shen, J.G. Zhao, W.S. Zhan, Appl. Phys. Lett. 71 (1997) 2727.
[25] K.Y. Wang, W.H. Song, J.M. Dai, S.L. Ye, S.G. Wang, J. Fang, J.L. Chen, B.J. Gao, J. J. Du, Y.P. Sun, J. Appl. Phys. 90 (2001) 6263.

Second ordermagneticphasetransitionandscalinganalysisiniron doped manganiteLa0.7Ca0.3Mn1xFexO3 compounds

ORIGINALITY REPORT

18%	10%	15%	%
SIMILARITY INDEX	INTERNET SOURCES	PUBLICATIONS	STUDENT PAPERS

PRIMARY SOURCES

1	Belhadj, A.. "Effect of laser cutting on microstructure and on magnetic properties of grain non-oriented electrical steels", Journal of Magnetism and Magnetic Materials, 200301 Publication	1%
2	topics.aip.org Internet Source	1%
3	A. Das. "Critical exponents of Cr-containing Co-rich metallic glasses", Physical Review B, 03/1993 Publication	1%
4	Srinivasan, G.. "Static and high-frequency magnetic properties of Fe and Cr substituted lanthanum manganites", Journal of Magnetism and Magnetic Materials, 20000301 Publication	1%
5	J. C. Lin, P. Tong, L. Zhang, W. J. Lu, X. B. Zhu, Z. R. Yang, W. H. Song, J. M. Dai, Y. P. Sun.	1%

"Structural, magnetic, electrical transport properties, and reversible room-temperature magnetocaloric effect in antipervoskite compound AlCMn3", Journal of Applied Physics, 2010
Publication

6	cnsm.kaist.ac.kr Internet Source	<1%
7	dmse.jlu.edu.cn Internet Source	<1%
8	Yus Rama Denny, Soonjoo Seo, Kangil Lee, Suhk Kun Oh, Hee Jae Kang, Sung Heo, Jae Gwan Chung, Jae Cheol Lee, Sven Tougaard. "Effects of cation compositions on the electronic properties and optical dispersion of indium zinc tin oxide thin films by electron spectroscopy", Materials Research Bulletin, 2015 Publication	<1%
9	www.victoria.ac.nz Internet Source	<1%
10	www.yhs.xju.edu.cn Internet Source	<1%
11	M. Balli, P. Fournier, S. Jandl, M. M. Gospodinov. " A study of the phase transition and magnetocaloric effect in multiferroic La	<1%

MnNiO single crystals ", Journal of Applied Physics, 2014
Publication

12	Watanabe, T.. "Magnetoresistance and high-temperature resistivity of Bi"2"."1Sr"1"."9Ca"1"."0Cu"2O"8"+"@d single crystals", Physica C: Superconductivity and its applications, 199605 Publication	<1%
13	S. M. Yusuf. "Effect of Ga doping for Mn on the magnetic properties of La_{0.67}Ca_{0.33}MnO_{3}", Physical Review B, 08/2002 Publication	<1%
14	doc.rero.ch Internet Source	<1%
15	Jun Zhang. "Anomalous strain effect on magnetic properties of La1xBaxMnO3 epitaxial thin films", Surface and Interface Analysis, 08/2001 Publication	<1%
16	www.ias.ac.in Internet Source	<1%
17	www.ilt.kharkov.ua Internet Source	<1%
18	Chau, N.. "Structure, magnetic, magnetocaloric	

	and magnetoresistance properties of La"1"-"xPb"xMnO"3 perovskite", Physica B: Physics of Condensed Matter, 200304 Publication	<1%
19	L.J. de Jongh. "Experiments on simple magnetic model systems", Advances In Physics, 1/1/1974 Publication	<1%
20	kundoc.com Internet Source	<1%
21	www.nd.edu Internet Source	<1%
22	Ikebe, M.. "An evidence for strong phonon-conduction electron interaction from thermal transport anomaly in Nd"0"."5"0Sr"0"."5"0MnO"3", Physica B: Physics of Condensed Matter, 20000601 Publication	<1%
23	I. Kamoun. "Magnetic and electrical properties of the lacunar La0.7Ca0.3−x□xMnO3 and La0.7−x□xCa0.3MnO3 oxides", physica status solidi (c), 05/2004 Publication	<1%
24	Jun-Woo Park, Hyeon Seob So, Hye-Min Lee, Hyo-Joong Kim, Han-Ki Kim, Hosun Lee. "Transition from a nanocrystalline phase to an amorphous phase in In-Si-O thin films: The	<1%

correlation between the microstructure and the optical properties", Journal of Applied Physics, 2015
Publication

25	Rabindra Nath Mahato, K. Sethupathi, V. Sankaranarayanan, R. Nirmala. "Large magnetic entropy change in nanocrystalline Pr0.7Sr0.3MnO3", Journal of Applied Physics, 2010 Publication	<1%
26	ariadne.mse.uiuc.edu Internet Source	<1%
27	S. Poon. "Critical phenomena and magnetic properties of an amorphous ferromagnet: Gadolinium-gold", Physical Review B, 07/1977 Publication	<1%
28	M. Haug. "Phase Transitions in Ordered and Disordered Ferrimagnets. II. Experimental Results", physica status solidi (b), 11/01/1987 Publication	<1%
29	www.jstage.jst.go.jp Internet Source	<1%
30	www.ufrgs.br Internet Source	<1%
31	Li, B.. "Magnetic properties of Cr-Fe-Mn alloys", Journal of Magnetism and Magnetic Materials,	<1%

200901
Publication

32	Han, Zhida, Bin Qian, Qiang Tao, Jiajun Wang, Ping Zhang, Rongjing Cui, and Xuefan Jiang. "Effect of Mn substitution on the phase transition and magnetocaloric effect in Dy(Co1−xMnx)2 alloys", Journal of Alloys and Compounds, 2013. Publication	<1%
33	www.tphys.jku.at Internet Source	<1%
34	www.uohyd.ernet.in Internet Source	<1%
35	A. Fondado, J. Mira, J. Rivas. "Power-law decay in first-order relaxation processes", Physical Review B, 2005 Publication	<1%
36	Yan, L.-q.. "Magnetic-field-induced transition from metastable spin glass to possible antiferromagnetic-ferromagnetic phase separation in Cd"0"."5Cu"0"."5Cr"2O"4", Journal of Magnetism and Magnetic Materials, 200907 Publication	<1%
37	Tapas Samanta. "Giant magnetocaloric effect in antiferromagnetic ErRu[sub 2]Si[sub 2] compound", Applied Physics Letters, 2007 Publication	<1%

38	www.springerprofessional.de Internet Source	<1%
39	Ihsan, Mohammad, Qing Meng, Li Li, Dan Li, Hongqiang Wang, Kuok Hau Seng, Zhixin Chen, Shane J. Kennedy, Zaiping Guo, and Hua-Kun Liu. "V2O5/Mesoporous Carbon Composite as a Cathode Material for Lithium-ion Batteries", Electrochimica Acta, 2015. Publication	<1%
40	Sangeetha, M., and V. Hari Babu. "Effect of yttrium substitution on the electrical and magnetic properties of La0.7Ba0.3MnO3 compound", Journal of Magnetism and Magnetic Materials, 2015. Publication	<1%
41	repositorio.unicamp.br Internet Source	<1%
42	Sudhakar, N.. "Room temperature ferromagnetism and magnetotransport properties of the layered manganite system La"1"."2Ba"1"."8Mn"2"-"xRu"xO"7 (0@?x@?1.0)", Solid State Communications, 200706 Publication	<1%
43	oacis.repo.nii.ac.jp Internet Source	<1%
44	uad.portalgaruda.org	

	Internet Source	<1%
45	Kim, K.S.. "The substitution effect of boron on reentrant behavior of rapidly solidified Fe-Mn-Zr alloys", Materials Science & Engineering A, 20070325 Publication	<1%
46	Nanto, Dwi, Zhang Peng, Yong-Yeal Song, Seong-Cho Yu, Sergey Telegin, Ludmila Elochina, and Andrey Telegin. "Magnetocaloric Effect and Refrigerant Capacity of Non-Stoichiometric ${\rm Nd}_{0.5}{\rm Sr}_{0.5}{\rm MnO}_{3}$ Single Crystalline", IEEE Transactions on Magnetics, 2012. Publication	<1%
47	authors.library.caltech.edu Internet Source	<1%
48	www.mpedram.com Internet Source	<1%
49	www.lib.kobe-u.ac.jp Internet Source	<1%
50	Cuong, T.D.. "Magnetism and related phenomena in RE(Co"1"-"xSi"x)"2 compounds", Journal of Alloys and Compounds, 19971114 Publication	<1%
	R. Rennie. "Geometry and topology of chiral	

51	anomalies in gauge theories", Advances In Physics, 11/1/1990 Publication	<1%
52	ir.lib.muroran-it.ac.jp Internet Source	<1%
53	Sharma, V.K.. "Investigations on the effect of gaseous environment during synthesis on the magnetic properties of Mn-doped ZnO", Journal of Alloys and Compounds, 20080630 Publication	<1%
54	mafiadoc.com Internet Source	<1%
55	Loudghiri, E.. "Magnetic properties of amorphous Gd"0"."6"7Y"0"."3"3", Physica B: Physics of Condensed Matter, 20041130 Publication	<1%
56	Fichera, D.. "Quantum field theories and critical phenomena on defects", Nuclear Physics, Section B, 20050808 Publication	<1%
57	D. Jérome. "Organic conductors and superconductors", Advances In Physics, 8/1/1982 Publication	<1%
58	Akhmad Zidni Hudaya, Arif Widyatama, Okto Dinaryanto, Wibawa Endra Juwana, Indarto,	<1%

Deendarlianto. "The liquid wave characteristics during the transportation of air-water stratified co-current two-phase flow in a horizontal pipe", Experimental Thermal and Fluid Science, 2019
Publication

59 L. Laroussi. "Low field magnetoresistance in La0.67Sr0.33-x□xMnO3 perovskite system", Phase Transitions, 1999 <1%
Publication

Exclude quotes	Off	Exclude matches	Off
Exclude bibliography	Off		